Article

Securing Non-Terrestrial FSO Link with Public Key Encryption Against Flying Object Attacks

Daniel Hicks [1], Fatma Benkhelifa [2], Zahir Ahmad [1], Thomas Statheros [3], Osama Saied [4], Omprakash Kaiwartya[4] and Farah Mahdi Alsallami [1]*

[1] The Faculty of Engineering, Environment and Computing, Coventry University, Coventry CV1 5FB, UK; hicksd2@uni.coventry.ac.uk, ad7175@coventry.ac.uk, ad9051@coventry.ac.uk
[2] School of Electronic Engineering and Computer Science, Queen Mary University of London, London E1 4NS, UK;fatma.benkhelifa@kaust.edu.sa
[3] The Centre for Future Transport and Cities, Coventry University, Coventry, CV1 2TE, UK;ac5304@coventry.ac.uk
[4] Department of Computer Science, Nottingham Trent University, Clifton Campus, NG11 8NS, UK;osama.saied@ntu.ac.uk, omprakash.kaiwartya@ntu.ed.ac
* Correspondence: ad9051@coventry.ac.uk

Abstract: Free Space Optical (FSO) communication has potential terrestrial and non-terrestrial applications. It allows large bandwidth for higher data transfer capacity. Due to its high directivity, it has a potential security advantage over traditional radio frequency (RF) communications. However, eavesdropping attacks are still possible in long non-terrestrial transmission FSO links, where the geometry of the link allows foreign flying objects such as Unmanned Aerial vehicles (UAVs) and drones to interrupt the links. This exposes non-terrestrial FSO links to adversary security attacks. Hence, data security techniques implementation is required to achieve immune FSO communication links. Unlike the commonly proposed physical layer security techniques, this paper presents a lab-based demonstration of a secured FSO communication link based on data cryptography using the Gnu-radio platform and software-defined radio (SDR) hardware. The utilized encryption algorithm (Xsalsa20) in this paper requires high-time complexity to be broken by power-limited flying objects that interrupt the FSO beam. The results show that implementing cryptographic encryption techniques into FSO systems provided resilience against eavesdropping attacks and preserved data security. The experiment results show that at a distance of 250 mm and laser output power of 10 mW, the system achieves a packet delivery rate of 92% and transmission rate of 10 Mbit/s. This is because the SDR used in this experiment requires a minimum received electrical amplitude of 27.5 mV to process the received signal. Long distance and higher data rates can be achieved using less sensitive SDR hardware.

Keywords: Data security; Free space optical communication; UAV; Non-Terrestrial Communication; Public Key Encryption.

Citation: Hicks D., Benkhelifa F., Ahmad Z., Statheros T., Saied O., Kaiwartya O. and Alsallami F. M. Securing Non-Terrestrial FSO Link with Public Key Encryption Against Flying Object Attacks. *Journal Not Specified* **2023**, *1*, 0. https://doi.org/

Received:
Revised:
Accepted:
Published:

1. Introduction

Free space optical (FSO) communication is one of the emerging breakthrough to support 6G networks. FSO links promise high data rates, licence-free spectrum, and massive connectivity. This technology supports fixed terrestrial point-to-point communication for military applications, mobile communications and internet service providers [1]. This system has also been proposed to provide non-terrestrial communication using satellite and unmanned aerial vehicles (UAVs) networks [2–4].

With any mode of FSO communication, terrestrial or non-terrestrial, it is crucial that sensitive information is kept secure. Due to the directional nature of optical beams, FSO is believed to offer superior security to radio frequency (RF) that makes it difficult to intercept [5,6]. For this reason, the literature related to physical layer security in wireless optical communications is scarce [5]. Although it is true, FSO offers more robust physical layer security than traditional RF transmissions, it is not a strong enough argument to disregard data security [5]. The study in [6] delves into physical layer security in FSO for the "difficulty of breach by a third party" compared to cryptographic techniques. Whilst this is true, it is also the case that physical layer encryption techniques often require additional hardware devices which drive the costs compared to mathematical cryptographic techniques at the presentation layer. To the best of our knowledge, none of the previous studies investigated this type of cryptographic encryption in FSO but instead focused on the physical layer.

Considering security is paramount to communication systems, literature on the presentation layer security is plentiful. Bernstein *et al.* highlights some of the underlying problems with cryptographic libraries such as OpenSSL and addressed them with a new library called Networking and Cryptography library (NaCl) (also known as salt). This library has some core features such as "No data flow from secrets to load addresses" and "centralizing randomness" to achieve higher performance and security. In [8], salt password hashing was used to secure data storage and transmission over a cloud computing network. The "salt" represents a random string which is hashed and combined with a hashed private key. The combination is once again hashed to guarantee the data cannot be decrypted under any condition. Similarly, [9] used salt cryptography to secure data transmissions by embedding the transmitted information into a video with promising results for how robust it is to attacks.

Likewise, more advanced data security techniques, such as elliptic curve cryptography, exist. In [10] the performance advantages of elliptic curve cryptography (ECC) were compared to other public key systems such as Rivest-Shamir-Adleman (RSA) or Diffie-Helman. The study concluded that the reason for ECC's success was due to industrial adaptation, which is as important as the performance advantages of a data security proposal. Recently, a non-terrestrial satellite or UAV-based FSO system whilst employing quantum key distribution (QKD) to secure the transmission was proposed in [11,12]. However, quantum-based security is cost ineffective because the technology is still in its infancy.

A balance of security and performance is important for adopting technologies such as FSO. It has been shown that strong upper-layer encryption techniques already exist and have been used to ensure secure data transmissions; however, they are not usually applied to a communication system using an FSO channel.

1.1. Motivation and original contributions

The most discussed advantage of FSO communication is that it allows huge bandwidths and data capacity, as demand is always growing in both the industrial and commercial sectors. However, eavesdropping attacks are possible when the transmission distance is large. For this reason, securing FSO links is essential to preserve the security of data and help with the adoption of new FSO technologies. Therefore, the main original contributions of this study are

- Implement a secure FSO link using the NaCl library to generate encryption keys in software using GNU Radio Companion (GRC) and investigate its performance in simulation. In particular, encryption algorithm (Xsalsa20) is used due to its high time complexity. Hence, it provides sufficient data security against adversary UAV that has limited computing power.
- Demonstrate a laboratory-based experiment of the secure FSO link using optics and software-defined radio (SDR) transceiver and compare results to the simulation.

The rest of the paper is organized as follows. The proposed system model is described in Section 3. Secure FSO link performance in GNU Radio simulation is discussed in Section 4. The experimental demonstration of the link is given in Section 5. Finally, conclusions are provided in Section 6.

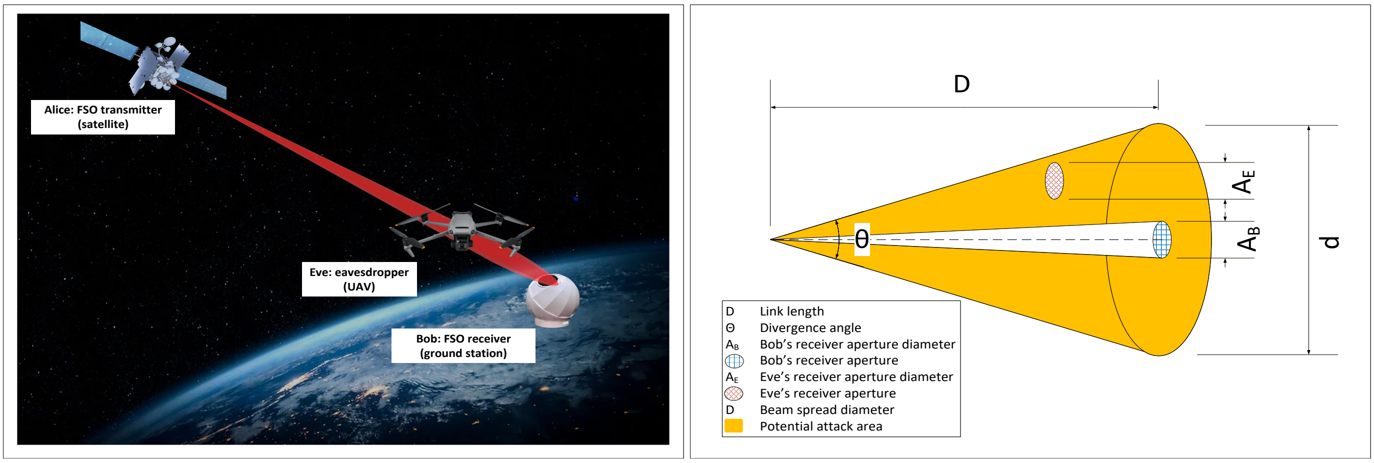

(a) (b)

Figure 1. Security attack on satellite to ground-station FSO link by a UAV that interrupts the optical beam: a) schematic (not to scale) and b) geometry of the link.

2. System Model

FSO is known for its narrow optical beam which offers immunity against security attacks. However, the beam spreads out with propagation distance, z, as follows [13,14]:

$$\omega(z) = \omega_\circ \sqrt{1 + \left(\frac{\lambda z}{\pi \omega_\circ^2}\right)^2} \tag{1}$$

where $\omega_\circ$ and λ are the beam waist and wavelength, respectively, of the laser at the transmitter.

Figure 1 shows a) schematic and b) geometry of a security attack scenario on a non-terrestrial FSO link between a satellite and ground station as the transmitter (Alice) and receiver (Bob), respectively. The attacker (Eve) is a UAV that interrupted the optical beam. The work in [15] showed that an FSO beam has a spread diameter $d \approx D\theta + R$ of 50 cm for a divergence angle of θ=0.1 mrad and link length of D =5 km, where R is the beam diameter at the transmitter. In satellite FSO communications, when the link length ranges from 500 km for low earth orbit satellites, to 500 million km for deep space optical links, the beam radius expands between 6.63 m to 2.19×10^5 m [16, P. 164]. This beam diameter expansion is 1000 times less than RF-based satellite communications beam [17,18] and it can be controlled using optics [19,20]. However, very narrow beam divergence is not desirable because it causes mis-alignment errors due to satellite vibration or platform jitter [17]. With the advances in UAV technologies, a flying attacker of 10 cm receiver aperture can interrupt the broad optical beam and align to the transmitter which exposes the FSO link to security threats [21], as illustrated in Figure 1b). In the terrestrial FSO case, Eve was assumed to be a sufficiently sensitive device that can collect a fraction of leak power $< 10^{-2}$, otherwise, it causes a power reduction that notifies the legitimate peers Alice and Bob [22]. The study in [22] also showed that relying on the physical layer security of the FSO is not sufficient when a fraction of leak power $> 10^{-2}$. Hence, an upper-layer data encryption technique is required.

In this study, we propose using a presentation layer data encryption technology to secure the transmission of non-terrestrial FSO communication links. Figure 2 illustrates a block diagram of the secure FSO system under investigation. The system is made in a simulation using the GNU Radio platform and as a prototype using an SDR transceiver and optical hardware. GNU Radio provides the user interface and handles the data processing for the transmitter and receiver in the background. The transmitter end allows a user to enter data to be encoded, encrypted, modulated, and shape burst. At the receiver end, the incoming data will be filtered, demodulated, decrypted, and decoded.

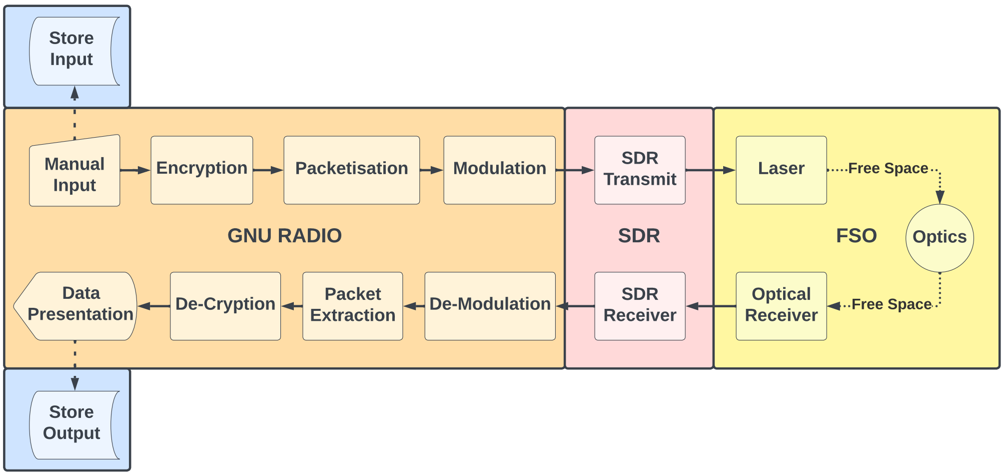

Figure 2. System block diagram.

The GNU-Radio module, responsible for implementing the encryption techniques, is an out-of-tree module called gr-nacl, developed by Wunsch *et al.*. This module uses a well-known library called NaCl that provides functions for high-speed network communication, encryption, and signatures [7,23]. This encryption technique has continuously proven to be secure despite advancements in modern computational power. The most efficient attack on the encryption algorithm (Xsalsa20), which is used in NaCl to generate encryption keys, showed that this technique only breaks 8 of 20 rounds of encryption with time complexity of 2^{250} [24]. This provides sufficient data security against power-limited eavesdroppers [25]. The NaCl library was implemented into this GNU Radio module using another library called libsodium [26]. It aims to wrap all the complex NaCl functions into simple high-speed calling functions. Finally, gr-nacl puts these functions into GNU Radio blocks that can be integrated with the rest of the workspace.

The NaCl cryptography library contains an abundance of algorithms and functions. However, only a handful of these has been implemented into gr-nacl: key generation, public encryption, private encryption, and stream encryption. We implemented public encryption techniques using the public encrypt/decrypt blocks and keypair generation blocks for both the sender and recipient.

Public encryption is used to avoid the need to exchange encryption keys across a secure channel. Moreover, this technique allow two parties to establish a secure channel by exchanging encryption keys across an insecure channel which is the case in non-terrestrial FSO.

3. Secure FSO link in GNU Radio simulation

The implementation of the secure FSO link in the GNU Radio platform is split into four main parts: the initial setup, the transmitter, the FSO channel and finally, the receiver. Each part is explained as follows:

3.1. Initialisation

Before any communication can occur, the initial setup must take place; this includes setting variables in GNU Radio for system parameters, as illustrated in Figure 3. There are also QT graphical user interface (GUI) blocks that control the user interface (UI) elements of the flowgraph. The QT GUI Range blocks allow the user to change the value of certain aspects of the FSO link using a slider and the QT GUI Tab widgets allow the user to switch between tabs for different system performance views.

At this stage, the encryption keys are generated, one pair for each transmitter and receiver. The Generate Keypair block uses a NaCl function called crypto_box_keypair to

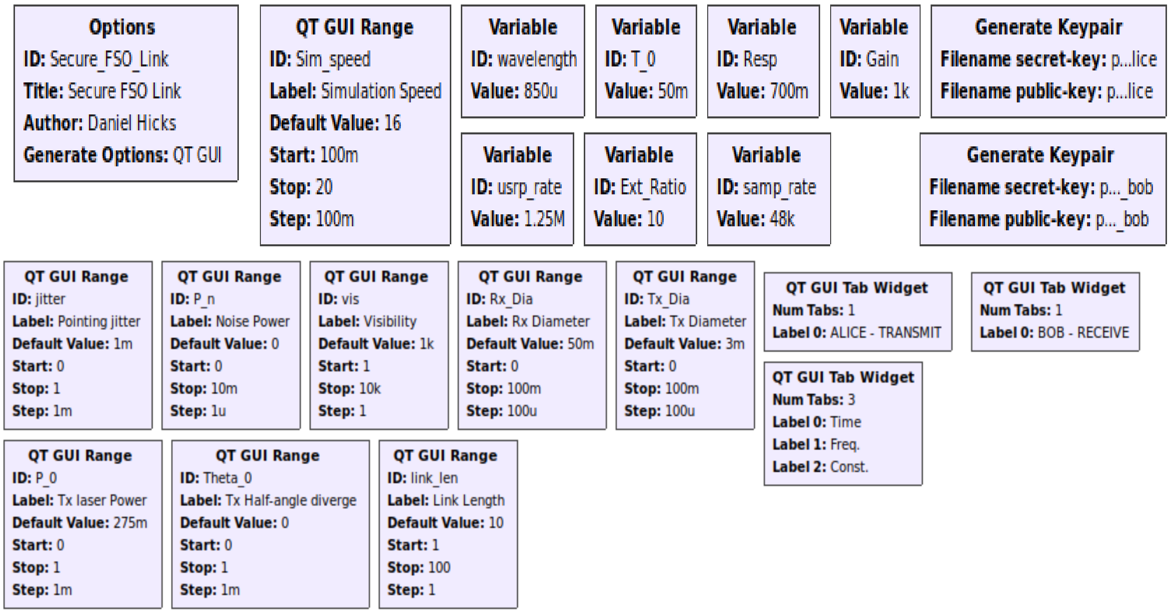

Figure 3. Secure FSO Initialisation blocks in GNU Radio.

generate a 32-byte secret key and a corresponding 32-byte public key. These random keys are generated using the Curve25519 function in NaCl which is a high-speed key generation method resulting in smaller keys than other cryptography methods such as RSA. The function first generates a random 32-byte integer which is considered to be private key, then computes a corresponding public key, the properties of elliptic curves are used to combine a base point with the random private key to produce the public key. Here, the curve used in Curve15519 is always defined as $y^2 = x^3 + 486662x^2 + x$. This public key is created so that it is impossible to decipher the private key from the public key and base point without considerable computational effort.

For encryption to occur, the sender must have the recipient's public key and vice versa. Therefore, the system become more secure as an attacker needs to know both the sender and recipient's public keys, which means the public keys can be exchanged across an insecure channel. In the case of this simulation, it is important to point out that this key exchange is assumed to have already taken place because the keys are stored on the same local drive. In the real world, the keys would have to be generated and then the public keys need to be exchanged for any secure communication to occur.

3.2. Transmitter

Once the initialisation stages are complete, the transmitter can send secured messages. There are six main stages that the transmitter goes through to prepare the message to be sent through free space, as depicted in Figure 4.

The first stage is for the user to enter a message into a UI entry box. Next, the message is passed to the custom message handler and the UI entry box is cleared; this message handler is coded specifically for this system. The message handler prepares the message format for encryption, clears the UI entry box, prints to the terminal, and stores the message in a log.

Therefore, GNU Radio passes asynchronous messages using streams. When the data is a message type (shown by blocks with grey inputs/outputs), the transferred data will be a polymorphic type (PMT). PMTs are commonly used for asynchronous communications due to their flexibility. The incoming message is a PMT and it gets converted to a PMT vector of 2 elements. The first element is the tag 'msg_clear'; this is needed as the encryption block searches for PMT vectors with the tag 'msg_clear' so that it can encrypt the second

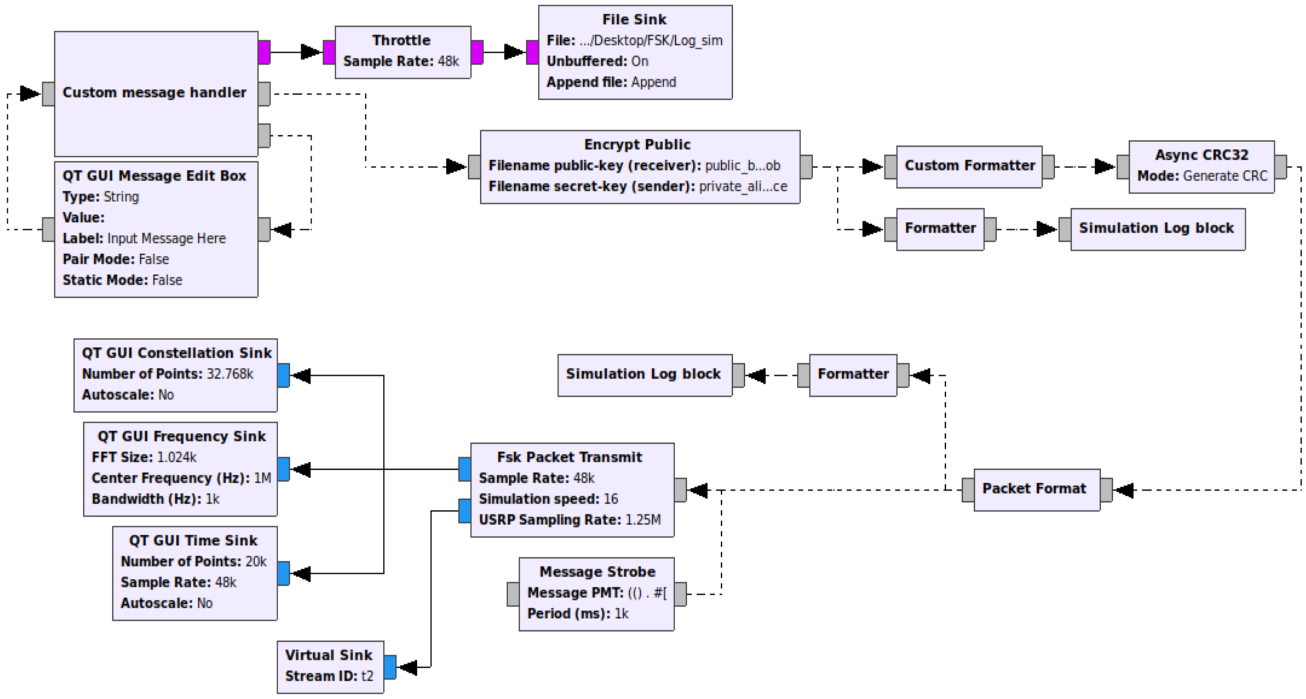

Figure 4. Secure FSO link Transmitter blocks in GNU Radio.

element of the vector, which contains the u8vector data of the message and is coupled with the metadata of its length. The message must be in this format for the encryption blocks to recognise the data and perform accurate encryption. The message is also stored in a log file and written to the terminal as part of the UI to debug the data flow.

Now the message is ready to be encrypted. The libsodium library provides a high-level application programming interface (API) for encryption that will produce an authenticated and encrypted message in one function. The function used by gr-nacl public encryption is crypto_box_easy, which takes a message, a random nonce, the sender's secret key and the recipient's public key to produce an encrypted message bundled with an authentication tag which ensures the message has not been tampered during transmission. The type of encryption used is called Xsalsa20 and the authentication used is Poly1305 [27].

The message is passed through another custom formatter block to change the message type to a PMT construct, containing the nonce and packet in u8vector form. Simultaneously the message is saved to the log and printed to the terminal by the formatter and subsequent simulation log block. Next, a 32-bit CRC is calculated and appended to the end of the message, which further ensures the integrity of the message at the receiver. One more custom formatter block applies a custom packet format that wraps the payload with 4-bytes of pre-amble, a 4-byte access code and finally four header bytes. For this work, the preamble is equal to 0×55 0×55 0×55 0×55 in hex or 85 85 85 85 in decimal and the access code is 0×E1 0×5A 0×E8 0×93 in hex or 225 90 232 147 in decimal. The final message configuration is ready to be sent to the transmitter for modulation, so once again it is saved to the log and written to the terminal. (Note that a message strobe block is also added here to keep the simulation active and push messages through certain buffers).

This message is passed to the frequency shift keying (FSK) packet transmit a hierarchal block of the gr-control out-of-tree (OOT) [28] module but has been modified to suit the proposed system. A complex voltage control oscillator (VCO) is used and a fractional resampler has been added to control the speed of the simulation by changing the resampling radio.

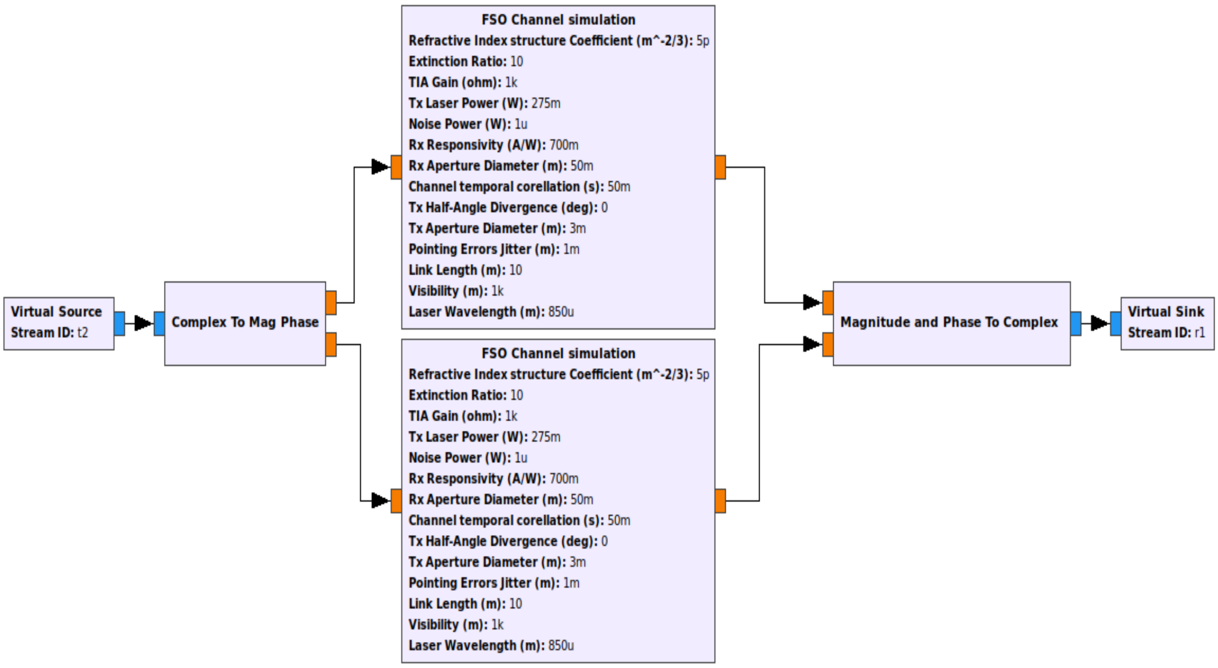

Figure 5. Secure FSO link Channel blocks in GNU Radio.

Now that the data has been modulated, it can be transmitted through the channel. Constellation, frequency, and time sinks are added after modulation as GUI elements to help visualise the signal and measure signal strength.

3.3. Channel

FSO systems are prone to random channels, and hence, received power varies due to atmospheric conditions such as fog and turbulence losses [29]. In addition, other sources of randomness occur due to link geometry, such as pointing errors and geometric losses. This can become problematic for the receiver. To simulate an accurate free space optical channel, an OOT module in [30] was used. The FSO channel is implemented using hierarchal blocks as shown in Figure 5. The FSO channel blocks account for channel variables that can be adjusted and tested in simulation.

The output of the packet transmit block is complex. However, FSO channel only allows real float vectors to pass through. The data type conversion methods in GNU Radio do not support direct complex to float conversion. Alternatively, to deal with this, the transmitted data must be split into its individual magnitude and phase samples and then passed through identical channels before being combined back into a single complex sample.

There are a total of eight channel variables to simulate four types of losses: geometric, turbulence, pointing errors and weather. Geometric losses describes the beam spreads over a distance as in (1); hence, not all the light from the transmitter can be focused onto the receiver. The amount of power lost from this is affected by the transmitter/receiver diameters, the link length and the transmitter half-angle divergence [19]. A higher divergence angle means the light spreads out more, and the receiver does not receive the full power. As the link length increases, the beam will also spread out more, meaning the receiver power will be lower [20].

Turbulence losses are a type of optical loss, caused by slight fluctuations in humidity, pressure and temperature in the air [31]. These losses are negligible in a lab environment but can have a significant impact over a longer distance in free space. For that reason, the simulated turbulence losses are also assumed to be small. The variables that will change

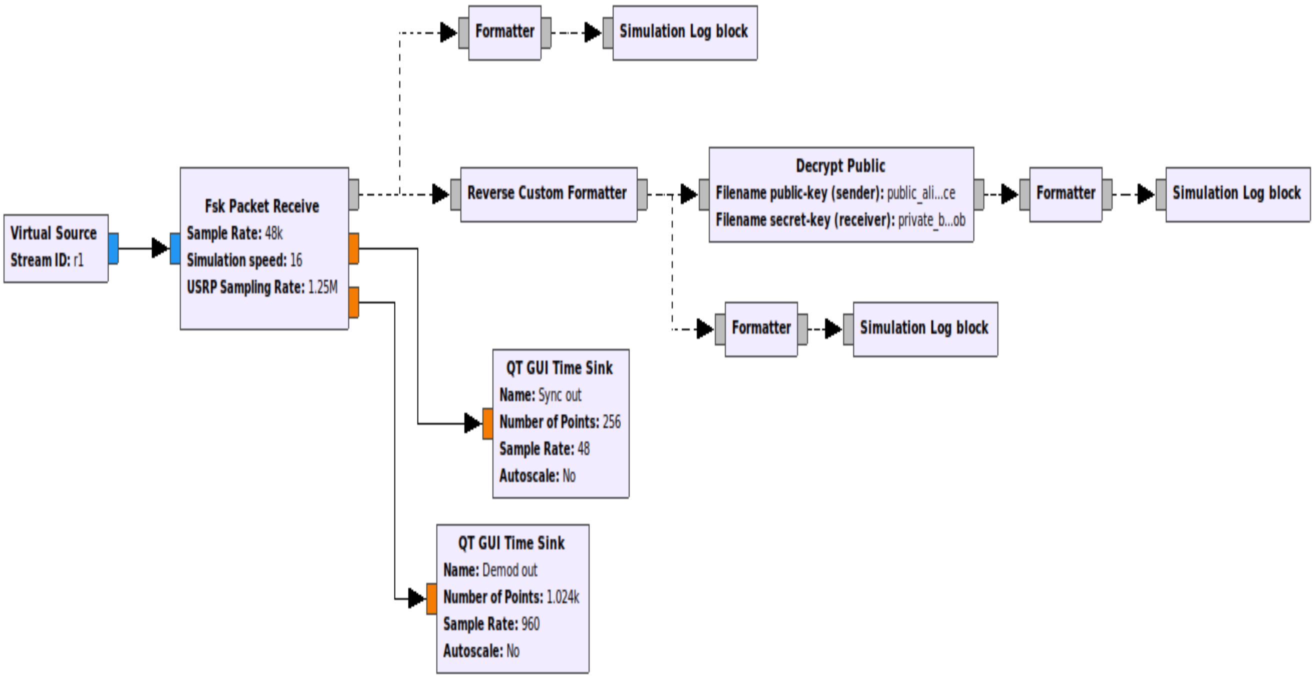

Figure 6. Secure FSO link Receiver blocks in GNU Radio.

the amount of loss are the refractive index and the channel temporal correlation; however, increasing the link length will also increase losses.

Pointing errors are affected by the alignment between the transmitter and receiver. This type of error is caused by the Jitter variable, which determines how far the centre of the beam can deviate from the centre of the receiver. It is caused by mechanical vibrations or a swaying structure [31]. Other factors, such as the link length, transmitter/receiver diameter and divergence angle, will change how much the jitter affects the final signal strength. For example, a longer link length will amplify these jitters at the receiver. Pointing errors are also negligible in a lab environment, so the pointing error jitter is kept at 0 in the simulation.

Weather losses, or fog losses, refer to losses caused by microscopic particles in the air (usually water droplets) that can reflect or block small parts of the beam and reduce the overall received power at the receiver. These losses are amplified over larger distances and are usually a major hurdle in industrial applications where air quality is lower [32]. However, in a lab, these losses are much less of a problem. The visibility variable has the utmost effect on the weather losses; however, as with other losses, the link length also changes the weather losses.

Each of these variables can be adjusted in the UI while the simulation is running by using a slider to make testing and data gathering as efficient as possible. Now that the data has passed through the simulated channel, depending on the values of the variables, noise is introduced, and the transmitted optical power decays. The receiver recovers the data from the noisy signal so that it can demodulate and decipher the important data from the packet.

3.4. Receiver

The receiver has the same stages as the transmitter but in reverse, as given in Figure 6. The data coming into the receiver must first pass through the FSK Packet Receive block before being depacketised and decrypted.

As explained in section 3.2, the access code is part of the header that consists of 4-bytes. The FSK Packet Receive block locates and discard the access code and any data before it (this includes the preamble). Then, it passes the rest of the binary data to the next block. Lastly, the bits are repacked into bytes and then the CRC is verified and passed on. Now the data will consist of just the nonce data and the encrypted packet data.

To extract the packet data and prepare the data for decryption, a reverse custom formatter was created. The reverse custom formatter will add the tag 'nonce' to the nonce data and pack it into a PMT list, and the encrypted message gets the tag 'msg_encrypted' and also gets packed into a PMT list, this is so that the decryption block locates the nonce and the encrypted data.

Next, the message is verified and decrypted by the Decrypt Public block from gr-nacl using the crypto_box_open_easy function from libsodium. If the message is properly decrypted, then the message is sent to the formatter to be written to the log, and it is also written to the terminal. If the message is not decrypted, then the bloc returns a message to indicate that the message cannot be decrypted and provide a reason, e.g., no nonce detected or the encryption key was invalid. In the last stage, the message is logged before the reverse formatter, after the reverse formatter and finally, after the decryption.

3.5. Simulation results

The communication link in simulation has been designed to replicate a realistic lab environment. The simulation parameters of the link are link length = 0.5m, receiver diameter = 4mm, transmitter diameter = 3mm and transmitter laser power = 10mW. The laser's half-angle divergence is assumed to be very small (very close to 0) due to the short link length and use of lenses that collimates the beam. System performance is measured by packet delivery rate (PDR) which is the ratio of the received packet number to the transmitted packet number.

Figure 7 shows the FSO link output of a secure conversation between Alice and Bob. The output shows a different format of the encrypted and packetized message at Alice and Bob. For example, the difference between an encrypted message and an encrypted packet is that the nonce and message have been combined into one and at the start of the message the 4-byte preamble is added (85 85 85 85), 4-byte sync is added (225 90 232 147), 4 header bytes are added.

In an eavesdropping attack, Eve can receive the data by using the same demodulation as Bob. Eve can also generate their keypair using the same method as Alice and Bob to decrypt the incoming messages using their private key and the sender's (Alice) public key. However, since Eve does not have the correct private encryption key, they cannot decrypt the gathered data.

Figure 8 shows that Eve has successfully received the message and can decipher the packet format. Eve can also identify the nonce and message begin but they cannot decrypt the message. The crypto_box_open_easy function from libsodium returns -1 "Failed to decrypt message." meaning the message cannot be decrypted and remains a secret.

To study the performance of the proposed system under realistic satellite to ground-station beam geometry and channel conditions, a simulation-based FSO link is implemented with realistic parameters shown in Table 1 [16] for low earth orbit satellite mission that uses miniature optical communication transceiver (MOCT) developed at the University of Florida. Figure 9 a) shows that this FSO link achieves a PDR of 88%. When the transmitted laser power is reduced to 0.1 W (i.e., a fraction of leakage power 10^{-2} [22]), the PDR decreases to 0%, unless Eve is 100x more sensitive or can boost the received signal using an amplifier with gain of 20 dB. In this case, the PDR increases to 96% as illustrated in Figure 9 b). The results also showed that Eve failed to decrypt any encrypted messages.

4. Secure FSO link experimental demonstration

Now that a secure FSO link has been demonstrated within a simulation, it can be moved to an FSO link prototype using optics and transceiver hardware. The aim is to replicate the parameters of the simulation in real life and compare the results of the

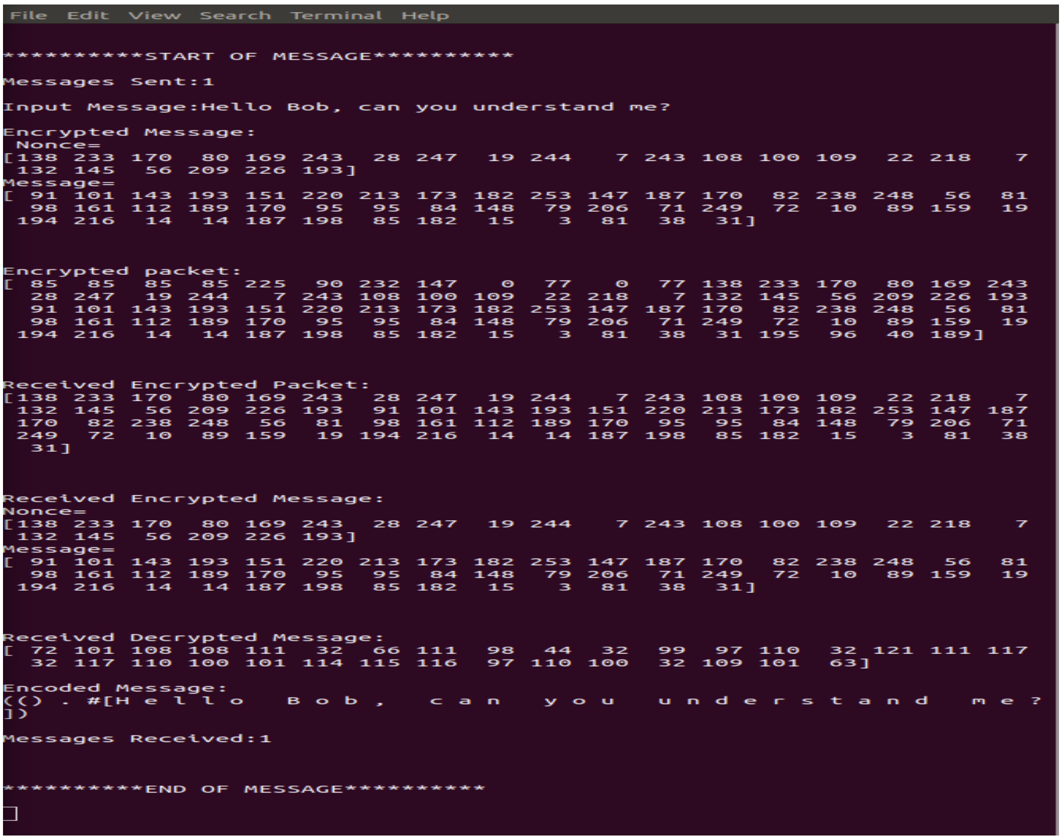

Figure 7. FSO link output of a secure conversation between Alice and Bob under ideal channel conditions.

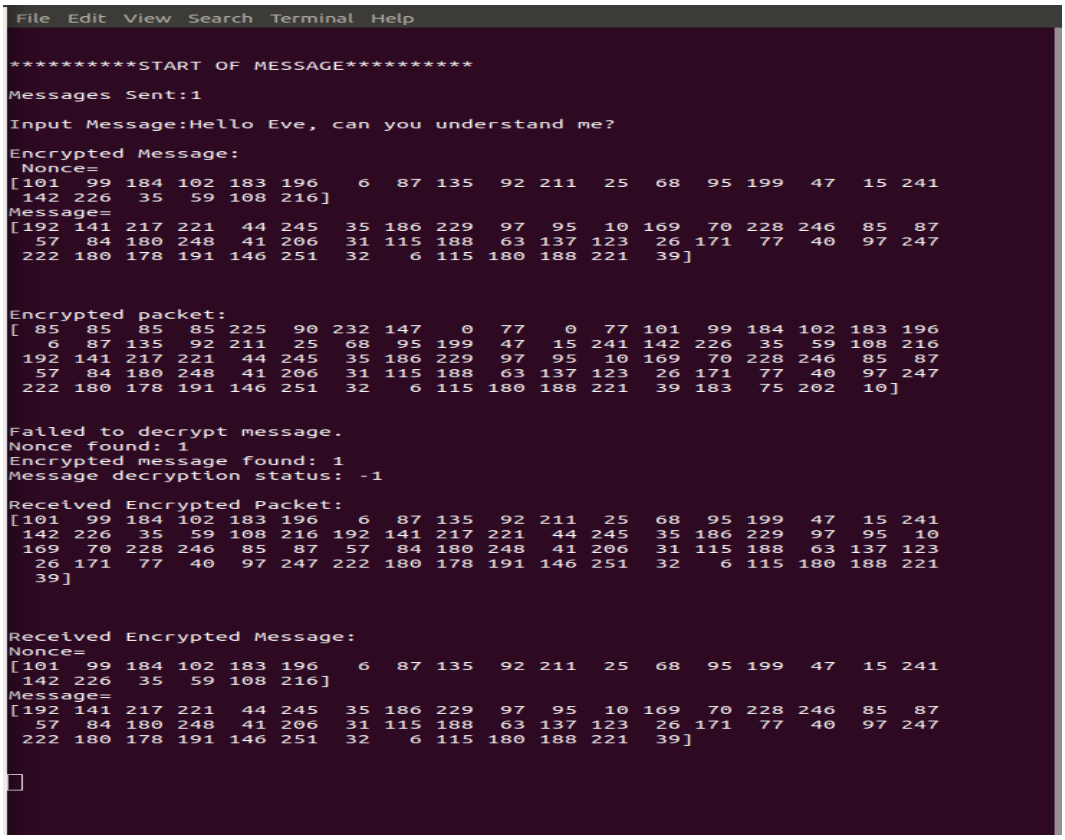

Figure 8. FSO link output of a secure conversation between Alice and Bob under ideal channel conditions.

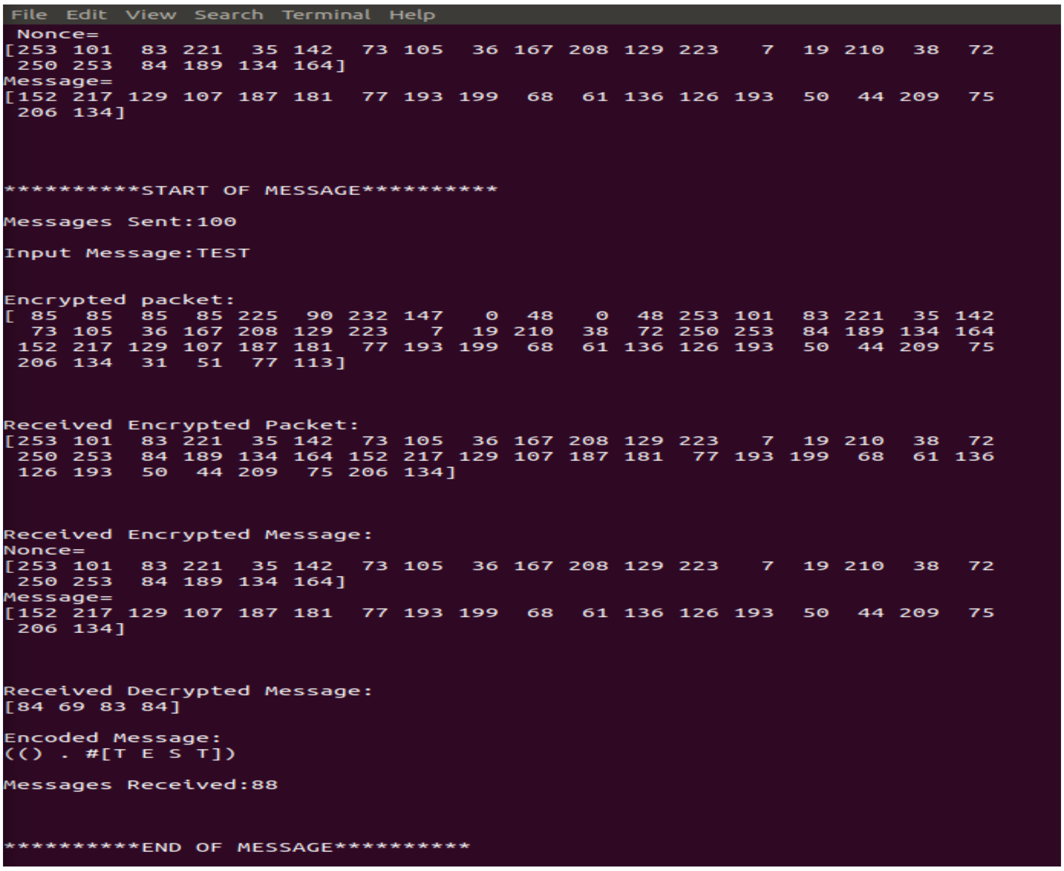

```
File  Edit  View  Search  Terminal  Help
 Nonce=
[253 101  83 221  35 142  73 105  36 167 208 129 223   7  19 210  38  72
 250 253  84 189 134 164]
Message=
[152 217 129 107 187 181  77 193 199  68  61 136 126 193  50  44 209  75
 206 134]


**********START OF MESSAGE**********

Messages Sent:100

Input Message:TEST

Encrypted packet:
[ 85  85  85  85 225  90 232 147   0  48   0  48 253 101  83 221  35 142
  73 105  36 167 208 129 223   7  19 210  38  72 250 253  84 189 134 164
 152 217 129 107 187 181  77 193 199  68  61 136 126 193  50  44 209  75
 206 134  31  51  77 113]


Received Encrypted Packet:
[253 101  83 221  35 142  73 105  36 167 208 129 223   7  19 210  38  72
 250 253  84 189 134 164 152 217 129 107 187 181  77 193 199  68  61 136
 126 193  50  44 209  75 206 134]


Received Encrypted Message:
Nonce=
[253 101  83 221  35 142  73 105  36 167 208 129 223   7  19 210  38  72
 250 253  84 189 134 164]
Message=
[152 217 129 107 187 181  77 193 199  68  61 136 126 193  50  44 209  75
 206 134]


Received Decrypted Message:
[84 69 83 84]

Encoded Message:
(() . #[T E S T])

Messages Received:88


**********END OF MESSAGE**********
```

(a)

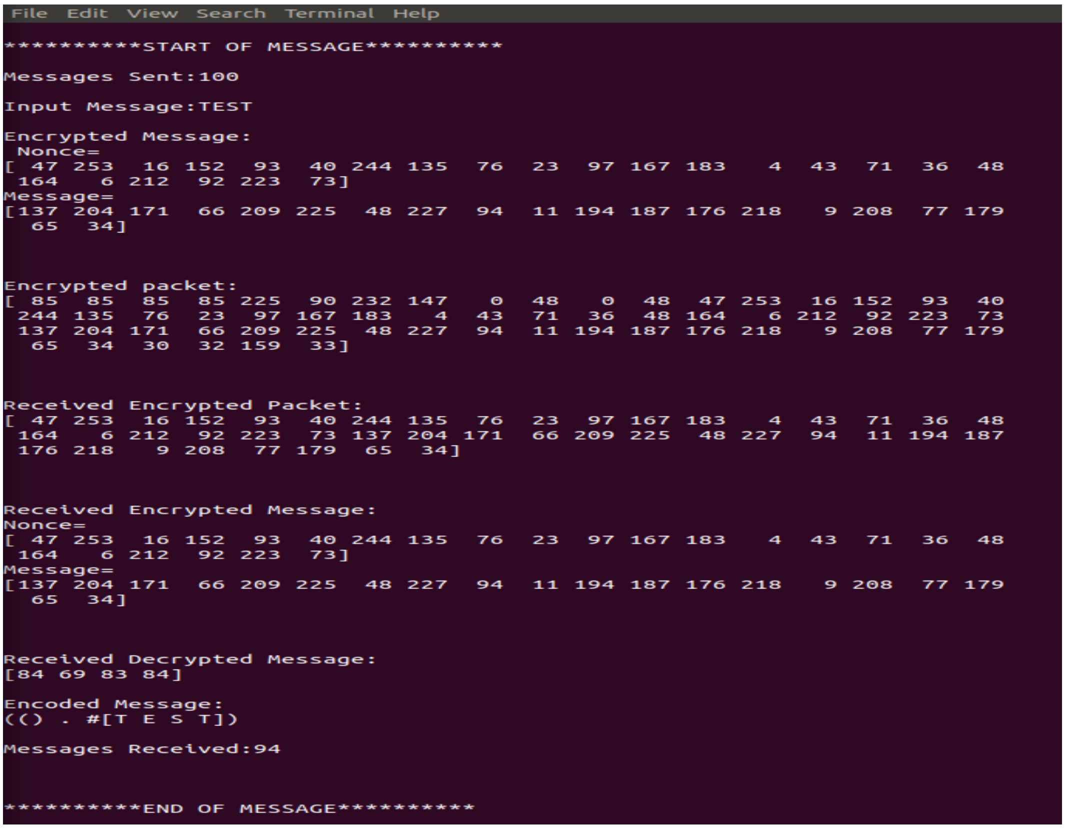

```
File  Edit  View  Search  Terminal  Help

**********START OF MESSAGE**********

Messages Sent:100

Input Message:TEST

Encrypted Message:
 Nonce=
[ 47 253  16 152  93  40 244 135  76  23  97 167 183   4  43  71  36  48
 164   6 212  92 223  73]
Message=
[137 204 171  66 209 225  48 227  94  11 194 187 176 218   9 208  77 179
  65  34]


Encrypted packet:
[ 85  85  85  85 225  90 232 147   0  48   0  48  47 253  16 152  93  40
 244 135  76  23  97 167 183   4  43  71  36  48 164   6 212  92 223  73
 137 204 171  66 209 225  48 227  94  11 194 187 176 218   9 208  77 179
  65  34  30  32 159  33]


Received Encrypted Packet:
[ 47 253  16 152  93  40 244 135  76  23  97 167 183   4  43  71  36  48
 164   6 212  92 223  73 137 204 171  66 209 225  48 227  94  11 194 187
 176 218   9 208  77 179  65  34]


Received Encrypted Message:
Nonce=
[ 47 253  16 152  93  40 244 135  76  23  97 167 183   4  43  71  36  48
 164   6 212  92 223  73]
Message=
[137 204 171  66 209 225  48 227  94  11 194 187 176 218   9 208  77 179
  65  34]


Received Decrypted Message:
[84 69 83 84]

Encoded Message:
(() . #[T E S T])

Messages Received:94


**********END OF MESSAGE**********
```

(b)

Figure 9. Simulation results of realistic satellite to ground-station FSO link parameters when the transmitter laser power values are: a) 10 W and b) 0.1 W and the receiver uses 20dB amplifier.

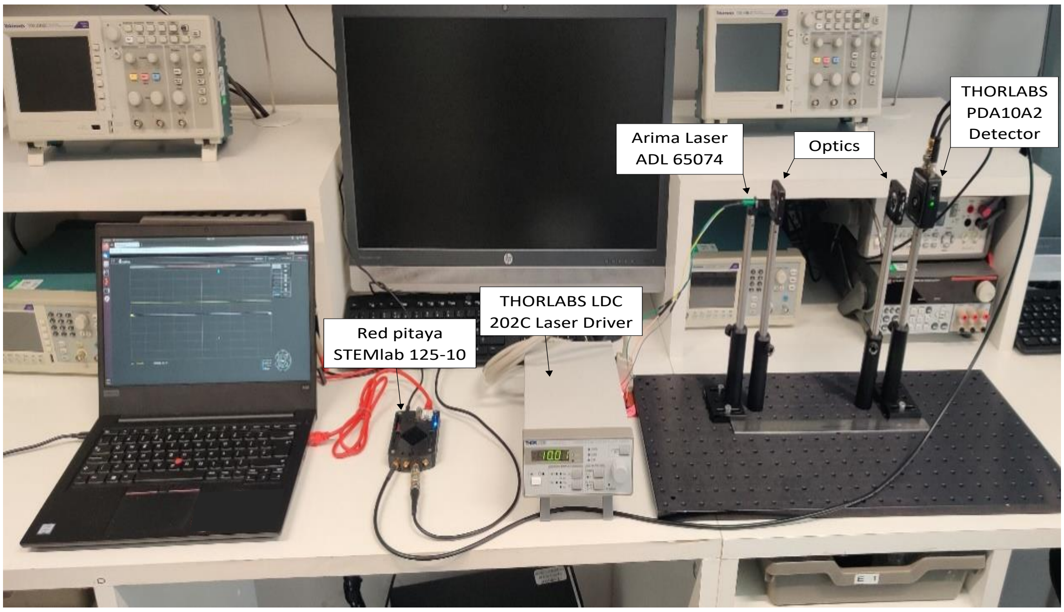

Figure 10. Secure FSO lab-based experiment setup.

Table 1. Satellite to ground-station link parameters for low earth orbit satellite mission that uses miniature optical communication transceiver (MOCT) developed at the University of Florida [16].

Parameter	Value
Link length	500000 m
Wavelength	1550 nm
Rx diameter	0.05 m
Tx diameter	0.005 m
Tx Half-angle diverge	0.133 mrad
Visibility range	1000 km
Pointing jitter	0.2 mrad

simulation and the physical FSO link. The encryption should hold up both in a simulation and a real environment for it to be considered secure.

4.1. Experiment setup

Figure 10 depicts the lab-based experiment setup of the secure FSO link. Red Pitaya SDR transceiver acts as the interface between the optical hardware and GNU Radio software in a loop-back connection. The host computer of GNU Radio communicates with the Red Pitaya's onboard FPGA via an Ethernet cable. Once the Red Pitaya processes the data through its digital-to-analogue converter (DAC), it is sent through the output RF port to the optical hardware. The optical hardware consists of a THORLABS LDC 202C laser driver, an Arima laser ADL 65074, 10mm focal length optics and a THORLABS PDA10A2 detector. The output of the Red Pitaya is connected to the modulation port of the laser driver. the driver modulates the power of the laser to match the output of the Red Pitaya. The laser driver also limits the laser current to 10mA to prevent any damage. The laser emits visible red light at 650nm, which is first collimated by an optic and then focused onto the receiver by a second optic of the same specification. By focusing the light correctly, a voltage of 60mV can be achieved at the optical receiver. The receiver will output a voltage, which can be connected straight into the input port of the Red Pitaya to be processed by its onboard digital down-converter (DDC) and sent, via Ethernet cable, to the GNU Radio interface.

Figure 11 shows the GRC file for the secure FSO link using the SDR and optical hardware. As explained in section 3, the implementation of the system in GNU Radio consists of four parts: the initial setup, the transmitter, the receiver, and the channel is

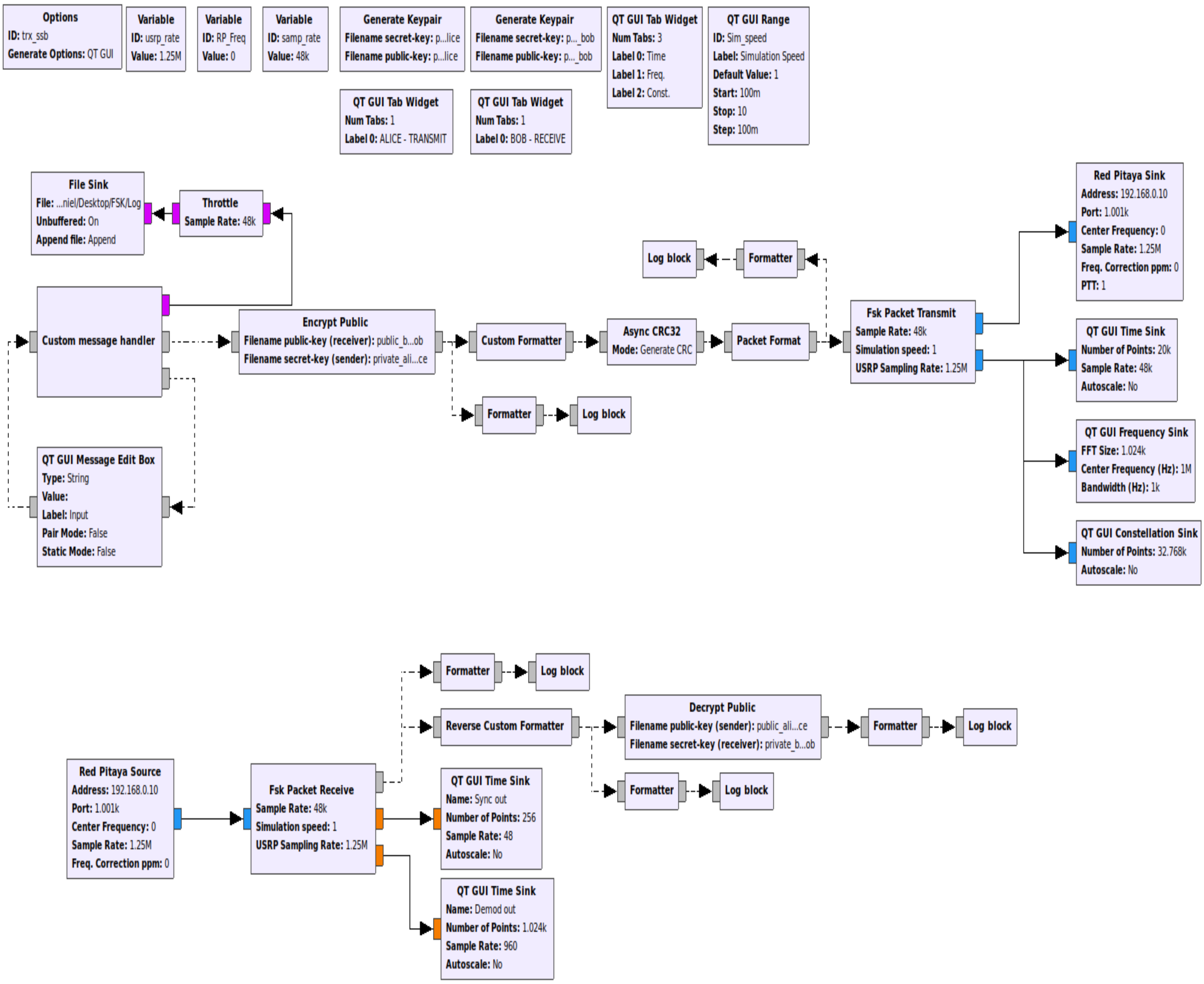

Figure 11. The GRC file for the secure FSO link using the optical hardware.

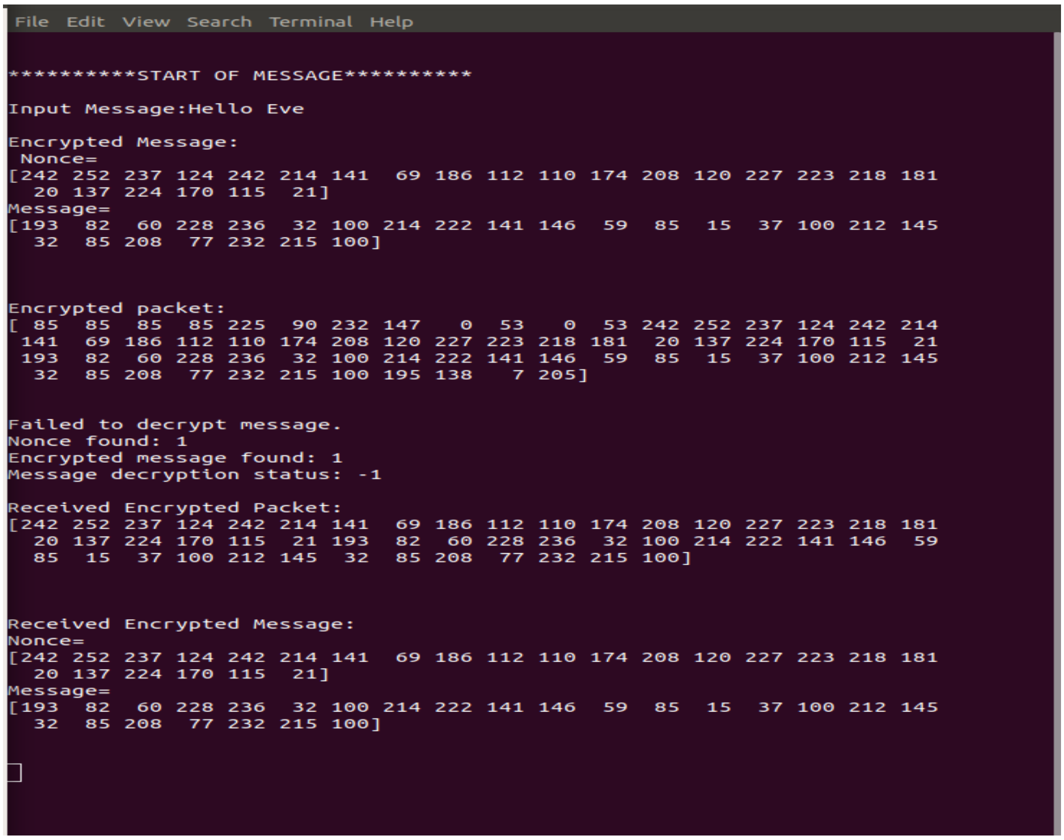

Figure 12. FSO link output under eavesdropping attacks.

replaced with hardware. The figure shows that the FSK packet transmitter and receiver are connected to the Red Pitaya sink and source, respectively, using the OOT blocks [33]. The Red Pitaya SDR acts as the interface between the optical hardware and GNU Radio software.

4.2. *Experiment results*

The experiment tested system resilience against eavesdropping attacks in the presence of Eve. Similar to section 3.5, Eve generated a private encryption key for the public decryption at the receiver. As shown in Figure 12, the decryption fails even if Eve can intercept the message and decode the header and packet data. This matches the results from the simulation and is the expected result due to the nature of the encryption. It can be concluded that the FSO link is reliable and secure against eavesdropping attacks.

The experiment results show that a distance of 250 mm between the transmitter and receiver achieves a minimum received electrical amplitude of 27.5 mV required at the Red Pitaya SDR to process the received signal. This achieves a PDR of 92%, as shown in Figure 13(a). While Figure 13(b) shows that reducing the distance to 130 mm increases the received electrical amplitude to 38.5 mV and the PDR to 96%.

Although communication speed is not the driving factor of this experiment, analysis was done to find the maximum achievable data rate. The communication speed can be changed by changing the sampling rate of the Red Pitaya, and taking fewer samples, which means a faster overall message speed. When the Red Pitaya samples the transmitter at 1.25 Mb/s, and since each byte sampled is made up of 8 bits (from 'init_u8vector' function during message formation), the achievable Red Pitaya transmission rate is 10 Mbit/s.

5. Discussion

This study considered a security attack scenario on a non-terrestrial FSO link between a satellite (Alice) and ground station (Bob). Due to the the long link length, the beam

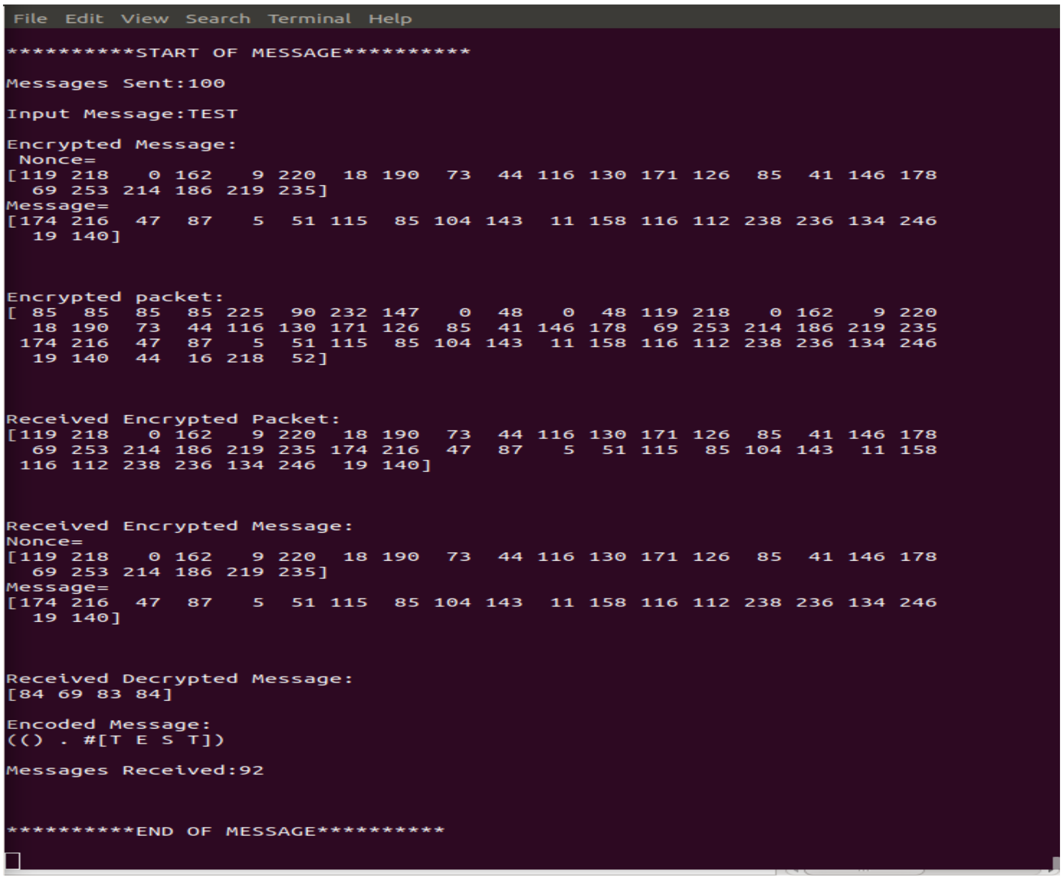

```
File  Edit  View  Search  Terminal  Help
**********START OF MESSAGE**********

Messages Sent:100

Input Message:TEST

Encrypted Message:
 Nonce=
[119 218   0 162   9 220  18 190  73  44 116 130 171 126  85  41 146 178
  69 253 214 186 219 235]
Message=
[174 216  47  87   5  51 115  85 104 143  11 158 116 112 238 236 134 246
  19 140]


Encrypted packet:
[ 85  85  85  85 225  90 232 147   0  48   0  48 119 218   0 162   9 220
  18 190  73  44 116 130 171 126  85  41 146 178  69 253 214 186 219 235
 174 216  47  87   5  51 115  85 104 143  11 158 116 112 238 236 134 246
  19 140  44  16 218  52]


Received Encrypted Packet:
[119 218   0 162   9 220  18 190  73  44 116 130 171 126  85  41 146 178
  69 253 214 186 219 235 174 216  47  87   5  51 115  85 104 143  11 158
 116 112 238 236 134 246  19 140]


Received Encrypted Message:
Nonce=
[119 218   0 162   9 220  18 190  73  44 116 130 171 126  85  41 146 178
  69 253 214 186 219 235]
Message=
[174 216  47  87   5  51 115  85 104 143  11 158 116 112 238 236 134 246
  19 140]


Received Decrypted Message:
[84 69 83 84]

Encoded Message:
(() . #[T E S T])

Messages Received:92


**********END OF MESSAGE**********
```

(a)

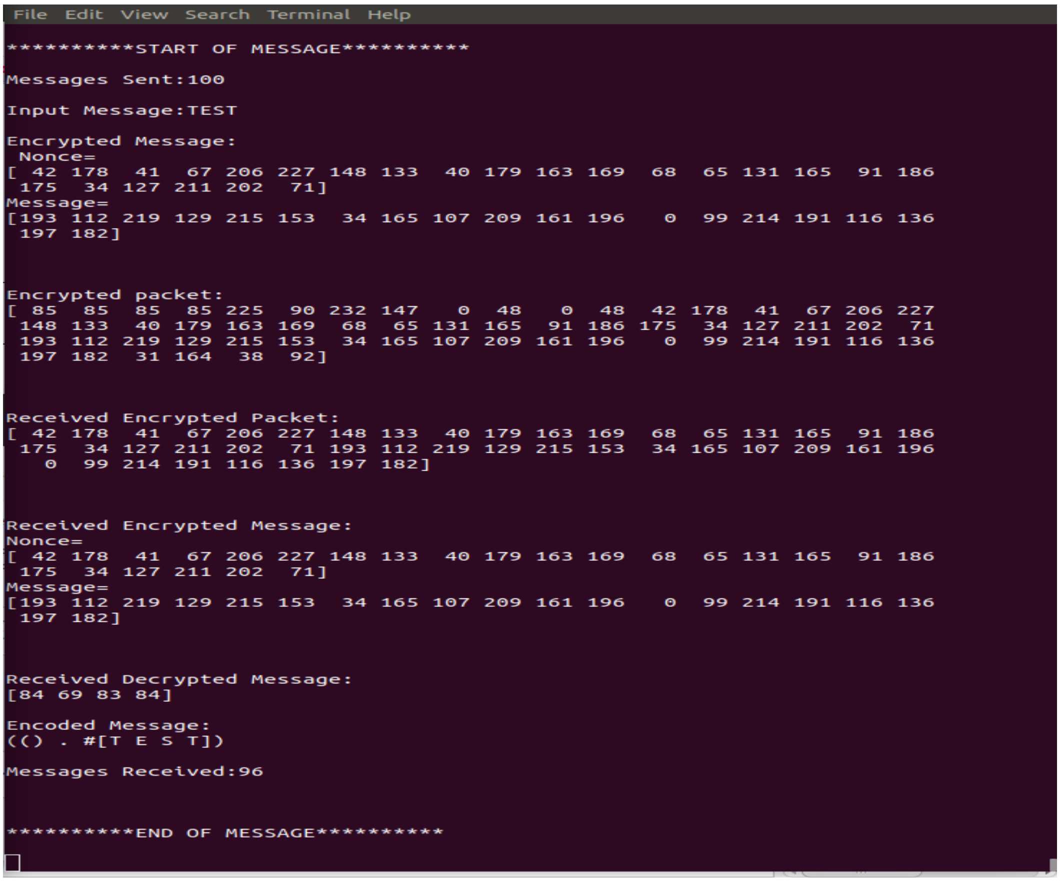

```
File  Edit  View  Search  Terminal  Help
**********START OF MESSAGE**********

Messages Sent:100

Input Message:TEST

Encrypted Message:
 Nonce=
[ 42 178  41  67 206 227 148 133  40 179 163 169  68  65 131 165  91 186
 175  34 127 211 202  71]
Message=
[193 112 219 129 215 153  34 165 107 209 161 196   0  99 214 191 116 136
 197 182]


Encrypted packet:
[ 85  85  85  85 225  90 232 147   0  48   0  48  42 178  41  67 206 227
 148 133  40 179 163 169  68  65 131 165  91 186 175  34 127 211 202  71
 193 112 219 129 215 153  34 165 107 209 161 196   0  99 214 191 116 136
 197 182  31 164  38  92]


Received Encrypted Packet:
[ 42 178  41  67 206 227 148 133  40 179 163 169  68  65 131 165  91 186
 175  34 127 211 202  71 193 112 219 129 215 153  34 165 107 209 161 196
   0  99 214 191 116 136 197 182]


Received Encrypted Message:
Nonce=
[ 42 178  41  67 206 227 148 133  40 179 163 169  68  65 131 165  91 186
 175  34 127 211 202  71]
Message=
[193 112 219 129 215 153  34 165 107 209 161 196   0  99 214 191 116 136
 197 182]


Received Decrypted Message:
[84 69 83 84]

Encoded Message:
(() . #[T E S T])

Messages Received:96


**********END OF MESSAGE**********
```

(b)

Figure 13. FSO link output at (a) 250mm and (b) 130mm distance

radius expands in the range of meters to kilometers. This beam radius expansion allows for UAV-born passive eavesdropper (Eve) to interrupt the broad optical beam without notifying the legitimate peers Alice and Bob under the hypotheses that Eve is sufficiently sensitive device that can collect a fraction of leak power $< 10^{-2}$ [22]. Hence, an upper-layer data encryption technique that uses the algorithm (Xsalsa20) within NaCl library where implemented to secure FSO systems. Gnu radio simulation platform with SDR hardware were used to prove the effectiveness of the proposed data encryption technique to prevent the eavesdropping.

Simulation results of a realistic non-terrestrial FSO link showed that when Eve receives a fraction of leak power $< 10^{-2}$ and boosts the received signal using an amplifier with gain of 20 dB, it can decipher the received packets with PDR of 96%. This is consistent with the literature [22] which reported a failure of the physical layer security to to prevent the eavesdropping at this level of leak power. The results also showed that Eve failed to decrypt any encrypted messages.

The immunity of the cryptographic encryption techniques to eavesdropping attacks was demonstrated experimentally using Gnu radio simulation platform with Red Pitaya SDR and optical hardware. The results also showed that combining encryption with FSO preserved data security.

The results of this study showed that more work is required to secure non-terrestrial optical communication systems. The proposed Xsalsa20 provides sufficient data security against flying eavesdropper that has limited computing power to break the key. However, advanced encryption techniques to prevent more powerful malicious security attacks with higher computing capability.

6. Conclusions

This study proposed implementing a secured FSO link for non-terrestrial communications against security attacks from flying objects. The system was tested in simulation and experimentally using the Gnu-radio platform and software-defined radio hardware. The results proved that implementing cryptographic encryption techniques using the algorithm (Xsalsa20) within NaCl library into FSO systems is effective at stopping eavesdropping attacks and preserving data security. The results also showed that at a distance of 250 mm, the secure system achieved a packet delivery rate of 92% and a transmission rate of 10 Mbit/s. This distance achieves a minimum received electrical amplitude of 27.5 mV required at the receiver SDR to process the data. Combining encryption with FSO helps the adoption of secure non-terrestrial optical communication systems. Xsalsa20 provides sufficient data security against flying eavesdropper that has limited computing power to break the key. More work needs to be done to implement advanced encryption techniques that will increase the versatility of this communication system.

Author Contributions: Conceptualization, D.Hicks and F. Alsallami; methodology, D.Hicks and F. Alsallami; software, D.Hicks ; formal analysis, D.Hicks; investigation, D.Hicks; resources, D.Hicks and F. Alsallami; data curation, D.Hicks; writing original draft preparation,D.Hicks and F. Alsallami; writing review and editing, F.Benkhelifa, Z.Ahmad, T.Statheros, O.Saied., O.Kaiwartya.; visualization, D.Hicks; supervision, F. Alsallami.

Funding: This research received no external funding.

Data Availability Statement: The data presented in this study are available on request from the corresponding author (ad9051@coventry.ac.uk). The data are not publicly available due to intellectual property rights.

Conflicts of Interest: The authors declare no conflict of interest.

References

1. Khalighi, M.A.; Uysal, M. Survey on Free Space Optical Communication: A Communication Theory Perspective. *IEEE Communications Surveys and Tutorials* **2014**, *16*, 2231–2258. https://doi.org/10.1109/COMST.2014.2329501.

2. Dong, Y.; Hassan, M.Z.; Cheng, J.; Hossain, M.J.; Leung, V.C.M. An Edge Computing Empowered Radio Access Network with UAV-Mounted FSO Fronthaul and Backhaul: Key Challenges and Approaches. *IEEE Wireless Communications* **2018**, *25*, 154–160. https://doi.org/10.1109/MWC.2018.1700419.
3. Lee, J.H.; Park, J.; Bennis, M.; Ko, Y.C. Integrating LEO Satellites and Multi-UAV Reinforcement Learning for Hybrid FSO/RF Non-Terrestrial Networks. *IEEE Transactions on Vehicular Technology* **2023**, *72*, 3647–3662. https://doi.org/10.1109/TVT.2022.3220696.
4. Chaudhary, S.; Amphawan, A. The Role and Challenges of Free-space Optical Systems. *Journal of Optical Communications* **2014**, *35*, 327–334. https://doi.org/doi:10.1515/joc-2014-0004.
5. Lopez-Martinez, F.J.; Gomez, G.; Garrido-Balsells, J.M. Physical-Layer Security in Free-Space Optical Communications. *IEEE Photonics Journal* **2015**, *7*, 1–14. https://doi.org/10.1109/JPHOT.2015.2402158.
6. Sato, Y.; Ikeda, K.; Koyama, O.; Yamada, M. Improving the quality of decrypted signal in an encryption system for secure free-space optical communication. In Proceedings of the 2019 24th Microoptics Conference (MOC), 2019, pp. 202–203. https://doi.org/10.23919/MOC46630.2019.8982752.
7. Bernstein, D.J.; Lange, T.; Schwabe, P. The security impact of a new cryptographic library. In Proceedings of the Progress in Cryptology–LATINCRYPT 2012: 2nd International Conference on Cryptology and Information Security in Latin America, Santiago, Chile, October 7-10, 2012. Proceedings 2. Springer, 2012, pp. 159–176.
8. Sajjan, R.S.; Ghorpade, V.R. Secure online encryption with partial data identity outsourcing: An exemplar for cloud computing. In Proceedings of the 2017 Fourteenth International Conference on Wireless and Optical Communications Networks (WOCN), 2017, pp. 1–8. https://doi.org/10.1109/WOCN.2017.8065841.
9. Sharma, N.; Rathi, R.; Jain, V.; Saifi, M.W. A novel technique for secure information transmission in videos using salt cryptography. In Proceedings of the 2012 Nirma University International Conference on Engineering (NUiCONE), 2012, pp. 1–6. https://doi.org/10.1109/NUICONE.2012.6493212.
10. Lauter, K. The advantages of elliptic curve cryptography for wireless security. *IEEE Wireless Communications* **2004**, *11*, 62–67. https://doi.org/10.1109/MWC.2004.1269719.
11. Alshaer, N.; Ismail, T. Performance Evaluation and Security Analysis of UAV-Based FSO/CV-QKD System Employing DP-QPSK/CD. *IEEE Photonics Journal* **2022**, *14*, 1–11. https://doi.org/10.1109/JPHOT.2022.3164355.
12. Vu, M.Q.; Le, H.D.; Pham, T.V.; Pham, A.T. Toward Practical Entanglement-Based Satellite FSO/QKD Systems Using Dual-Threshold/ Direct Detection. *IEEE Access* **2022**, *10*, 113260–113274. https://doi.org/10.1109/ACCESS.2022.3217220.
13. Kaymak, Y.; Rojas-Cessa, R.; Feng, J.; Ansari, N.; Zhou, M. On Divergence-Angle Efficiency of a Laser Beam in Free-Space Optical Communications for High-Speed Trains. *IEEE Transactions on Vehicular Technology* **2017**, *66*, 7677–7687. https://doi.org/10.1109/TVT.2017.2686818.
14. Wang, J.; Wang, G.; Bai, R.; Li, B.; Zhou, Y. Ground simulation method for arbitrary distance optical transmission of a free-space laser communication system based on an optical fiber nanoprobe. *Journal of Optical Communications and Networking* **2017**, *9*, 1136–1144. https://doi.org/10.1364/JOCN.9.001136.
15. Eghbal, M.; Abouei, J. Security enhancement in free-space optics using acousto-optic deflectors. *Journal of Optical Communications and Networking* **2014**, *6*, 684–694. https://doi.org/10.1364/JOCN.6.000684.
16. Barnwell, N. Free-Space Optical Links for Small Spacecraft Navigation, Timing, and Communication. PhD thesis, University of Florida Gainesville, FL, USA, 2018.
17. Kaushal, H.; Kaddoum, G. Optical Communication in Space: Challenges and Mitigation Techniques. *IEEE Communications Surveys and Tutorials* **2017**, *19*, 57–96. https://doi.org/10.1109/COMST.2016.2603518.
18. Franz, J.; Jain, V.K. *Optical communications, components and systems, analysis design optimization application*; 2000.
19. Najafi, M.; Schmauss, B.; Schober, R. Intelligent Reflecting Surfaces for Free Space Optical Communication Systems. *IEEE Transactions on Communications* **2021**, *69*, 6134–6151. https://doi.org/10.1109/TCOMM.2021.3084637.
20. Safi, H.; Dargahi, A.; Cheng, J.; Safari, M. Analytical Channel Model and Link Design Optimization for Ground-to-HAP Free-Space Optical Communications. *Journal of Lightwave Technology* **2020**, *38*, 5036–5047. https://doi.org/10.1109/JLT.2020.2997806.
21. Ortiz, G.G.; Lee, S.; Monacos, S.; Wright, M.; Biswas, A. Design and development of a robust ATP subsystem for the Altair UAV-to-Ground lasercomm 2.5 Gbps demonstration **2003**. https://doi.org/2014/7008.
22. Lopez-Martinez, F.J.; Gomez, G.; Garrido-Balsells, J.M. Physical-Layer Security in Free-Space Optical Communications. *IEEE Photonics Journal* **2015**, *7*, 1–14. https://doi.org/10.1109/JPHOT.2015.2402158.
23. Wunsch, S.; Müller, S.; Nieboer, G. gr-nacl: GNU Radio data encryption module, 2017. https://doi.org/https://github.com/stwunsch/gr-nacl.
24. Aumasson, J.P.; Fischer, S.; Khazaei, S.; Meier, W.; Rechberger, C. New Features of Latin Dances: Analysis of Salsa, ChaCha, and Rumba. In Proceedings of the Fast Software Encryption; Nyberg, K., Ed.; Springer Berlin Heidelberg: Berlin, Heidelberg, 2008; pp. 470–488.
25. Das, S.K.; Kant, K.; Zhang, N. *Handbook on Securing Cyber-Physical Critical Infrastructure*, 1st ed.; Morgan Kaufmann Publishers Inc.: San Francisco, CA, USA, 2012.
26. Denis, F. libsodium, 2017. https://doi.org/https://github.com/jedisct1/libsodium.
27. Bernstein, D.J.; Lange, T.; Schwabe, P. The Security Impact of a New Cryptographic Library. In Proceedings of the Progress in Cryptology – LATINCRYPT 2012; Hevia, A.; Neven, G., Eds.; Springer Berlin Heidelberg: Berlin, Heidelberg, 2012; pp. 159–176.

28. Duggan, B. gr-nacl: GNU Radio data encryption module, April 2022. https://doi.org/Gr-control.GitHub..https://github.com/duggabe/gr-control.
29. Htay, Z.; Ghassemlooy, Z.; Zvanovec, S.; Abadi, M.M.; Burton, A. An Experimental Testbed for Implementation and Validation of Software defined FSO under Atmospheric Conditions using USRPs. In Proceedings of the 2022 13th International Symposium on Communication Systems, Networks and Digital Signal Processing (CSNDSP), 2022, pp. 59–64. https://doi.org/10.1109/CSNDSP54353.2022.9908057.
30. Abadi, M.M. FSO-Comm-GnuRadio-Module, Oct 2019. https://doi.org/https://github.com/MansourM61/FSO-Comm-GnuRadio-Modulel.
31. Pang, W.; Wang, P.; Han, M.; Li, S.; Yang, P.; Li, G.; Guo, L. Optical Intelligent Reflecting Surface for Mixed Dual-Hop FSO and Beamforming-Based RF System in C-RAN. *IEEE Transactions on Wireless Communications* **2022**, *21*, 8489–8506. https://doi.org/10.1109/TWC.2022.3166756.
32. Htay, Z.; Ghassemlooy, Z.; Abadi, M.M.; Burton, A.; Mohan, N.; Zvanovec, S. Performance Analysis and Software-Defined Implementation of Real-Time MIMO FSO With Adaptive Switching in GNU Radio Platform. *IEEE Access* **2021**, *9*, 92168–92177. https://doi.org/10.1109/ACCESS.2021.3092968.
33. Demin, P. Red Pitaya Notes, March 2022. https://doi.org/https://github.com/pavel-demin/red-pitaya-notes.